Induced ferroelectric phases in $TbMn_2O_5$

P. Tolédano
Laboratory of Complex Systems, 33 rue Saint-Leu, University of Picardie, 80000 Amiens, France

W. Schranz and G. Krexner
Faculty of Physics, University of Vienna, Boltzmanngasse 5, A-1090 Vienna, Austria

(Received 2 October 2008; revised manuscript received 9 February 2009; published 2 April 2009)

The magnetostructural transitions and magnetoelectric effects reported in $TbMn_2O_5$ are described theoretically and shown to correspond to two essentially different mechanisms for the induced ferroelectricity. The incommensurate and commensurate phases observed between 38 and 24 K exhibit a hybrid pseudoproper ferroelectric nature resulting from an effective bilinear coupling of the polarization with the antiferromagnetic order parameter. This explains the high sensitivity of the dielectric properties of the material under applied magnetic field. Below 24 K the incommensurate phase shows a standard improper ferroelectric character induced by the coupling of two distinct magnetic order parameters. The complex dielectric behavior observed in the material reflects the crossover from one to the other transition regime. The temperature dependences of the pertinent physical quantities are worked out, and previous theoretical models are discussed.

DOI: 10.1103/PhysRevB.79.144103 PACS number(s): 77.80.−e, 61.50.Ah, 75.80.+q

I. INTRODUCTION

It was recently observed[1,2] that an electric polarization can emerge at a magnetic transition if the magnetic spins order in noncollinear spiral structures. This type of magnetostructural transition was reported in various classes of multiferroic materials,[3–6] such as the rare-earth manganites $RMnO_3$ (Ref. 7) and RMn_2O_5,[8,9] $Ni_3V_2O_8$,[10] $MnWO_4$,[11] $CoCr_2O_4$,[12] or Cr_2BeO_4.[13] In these compounds the correlation between spins and electric dipoles gives rise to remarkable magnetoelectric effects, indicating a strong sensitivity to an applied magnetic field, such as reversals or flops of the polarization, and a strong enhancement of the dielectric permittivity. In the aforementioned materials the ferroelectric phases appear below an intermediate nonpolar magnetic phase, i.e., the breaking of inversion symmetry, which allows emergence of ferroelectric properties, does not occur simultaneously with the breaking of time-reversal symmetry.

Theoretical arguments have been raised[14–18] to justify the observation of magnetoelectric effects in spiral magnets. However, a comprehensive theoretical description of the experimental results disclosed in multiferroic materials could not be achieved because the actual symmetries of the primary (magnetic) and secondary (structural) order parameters have not been related organically to the thermodynamic functions which provide the relevant phase diagrams. Here, we give a unifying theoretical description of the magnetostructural transitions found in the manganite $TbMn_2O_5$ (Refs. 8, 9, 19, and 20) in the framework of the Landau theory of magnetic phase transitions.[21–23] It reveals that the transitions observed in this compound at 38 and 24 K correspond to essentially different mechanisms for the induced ferroelectricity: The 38 K transition involves an *effective bilinear* coupling of the polarization with a *single* magnetic order parameter. It results in a *pseudoproper* ferroelectric nature for the phases stable between 38 and 24 K. By contrast, the 24 K transition exhibits an *improper* ferroelectric behavior corresponding to a linear-quadratic coupling of the polarization with *two distinct* magnetic order parameters. The crossover from one to the other transition mechanism provides an interpretation of the dielectric behavior observed in the absence or presence of an applied magnetic field.[8,9]

On cooling below the paramagnetic Pbam1′ (P) structure, $TbMn_2O_5$ undergoes five phase transitions[8,9] taking place successively at $T_1=43$ K, $T_2=38$ K, $T_3=33$ K, $T_4=24$ K, and $T_5=10$ K, the corresponding phases being denoted I–V. The paper is organized as follows: in Sec. II the $P\rightarrow I\rightarrow II\rightarrow III$ sequence of transitions giving rise at T_1, T_2, and T_3, to the incommensurate phases I and II, and commensurate phase III,[8,9] is described theoretically. The remarkable magnetoelectric effects occurring at the $III\rightarrow IV\rightarrow V$ transitions, taking place at T_4 and T_5, are analyzed in Sec. III. In Sec. IV our results are summarized and compared to the results obtained in previous theoretical works on $TbMn_2O_5$.[24–30] The applicability of our description to other RMn_2O_5 compounds[31–36] is outlined.

II. P→I→II→III TRANSITIONS

The wave vector associated with the incommensurate antiferromagnetic phase I and ferroelectric phase II is $\vec{k}=(1/2,0,k_z)$, with k_z decreasing from about 0.30 to 0.25. It is associated with a four-dimensional irreducible corepresentation (IC) of Pbam1′, denoted G_1, whose generators are given in Table I. The complex amplitudes $S_1=\rho_1 e^{i\theta_1}$, $S_1^*=\rho_1 e^{-i\theta_1}$, $S_2=\rho_2 e^{i\theta_2}$, and $S_2^*=\rho_2 e^{-i\theta_2}$ of the magnetic waves transforming according to G_1, form the symmetry-breaking order parameter for the $P\rightarrow I\rightarrow II$ transitions, giving rise to the invariants $\Im_1=\rho_1^2+\rho_2^2$, $\Im_2=\rho_1^2\rho_2^2$, and $\Im_3=\rho_1^2\rho_2^2\cos 2\theta$, with $\theta=\theta_1-\theta_2$. Therefore the homogeneous part of the free-energy density reads

$$\Phi_1(\rho_1,\rho_2,\theta)=a_1\Im_1+a_2\Im_1^2+b_1\Im_2+b_2\Im_2^2+c_1\Im_3+c_2\Im_3^2+d\Im_1\Im_3+\cdots. \quad (1)$$

An eighth degree expansion is required in order to account for the full set of stable phases resulting from the minimiza-

TABLE I. Generators of the IC's G_1, Ξ_1, and Ξ_2. Diagonal 4×4 matrices are represented by columns. A cross ($\times$) indicates that the matrix is the same as in the upper row. $\epsilon=k_z c$ except in the commensurate phase III where $\epsilon=\frac{\pi}{2}$. $\epsilon'=k_x\frac{a}{2}$. G_1 is deduced from the irreducible representation (IR) of the group $G_k=mm2$, denoted $\hat{\tau}_1(k_{16})$ in Kovalev's tables (Ref. 40). Ξ_1 and Ξ_2 are deduced from the IR's $[\hat{\tau}_1(k_3)$ and $\hat{\tau}_2(k_3)]$ of $G_k=m_y$. T is the time-reversal operation.

Pbam1′		$(U_z \mid 000)$	$(\sigma_x \mid \frac{a}{2}\frac{b}{2}0)$	$(I \mid 000)$	T	$(E \mid a00)$	$(E \mid 00c)$
G_1	S_1	$\begin{bmatrix}+1\\+1\\-1\\-1\end{bmatrix}$	$\begin{bmatrix}&&i&\\&&&-i\\-i&&&\\&i&&\end{bmatrix}$	$\begin{bmatrix}&1&&\\1&&&\\&&&1\\&&1&\end{bmatrix}$	$\begin{bmatrix}-1\\-1\\-1\\-1\end{bmatrix}$	$\begin{bmatrix}-1\\-1\\-1\\-1\end{bmatrix}$	$\begin{bmatrix}e^{i\epsilon}\\e^{-i\epsilon}\\e^{i\epsilon}\\e^{-i\epsilon}\end{bmatrix}$
	S_1^*						
	S_2						
	S_2^*						
Ξ_1	η_1	$\begin{bmatrix}&1&&\\&&&1\\1&&&\\&1&&\end{bmatrix}$	$\begin{bmatrix}&&e^{i\epsilon'}&\\&&&e^{-i\epsilon'}\\e^{-i\epsilon'}&&&\\&e^{i\epsilon'}&&\end{bmatrix}$	X	X	$\begin{bmatrix}e^{i\epsilon'}\\e^{-i\epsilon'}\\e^{i\epsilon'}\\e^{-i\epsilon'}\end{bmatrix}$	X
	η_1^*						
	η_2						
	η_2^*						
Ξ_2	ς_1	X	$\begin{bmatrix}&&-e^{i\epsilon'}&\\&&&-e^{-i\epsilon'}\\-e^{-i\epsilon'}&&&\\&-e^{i\epsilon'}&&\end{bmatrix}$	X	X	X	X
	ς_1^*						
	ς_2						
	ς_2^*						

tion of Φ_1 and for disclosing the magnetoelectric properties observed in $TbMn_2O_5$. It stems from the following rule demonstrated in Ref. 37: if n is the highest degree of the basic order-parameter invariants (here $n=4$ for the $\mathfrak{I}_2$ and $\mathfrak{I}_3$ invariants), the free energy has to be truncated at not less than the degree $2n$ (here $2n=8$) for ensuring the stability of all phases involved in the phase diagram. However, one can neglect most of the nonindependent invariants of degrees lower than or equal to eight (as for example $\mathfrak{I}_1^3$, $\mathfrak{I}_1^4$, $\mathfrak{I}_1\mathfrak{I}_2$, or $\mathfrak{I}_2\mathfrak{I}_3$) which can be shown to have no influence on the stability of the phases, but only modify secondary features of the phase diagram, as for example the shape of the transition lines separating the stable phases. In contrast the invariant $\mathfrak{I}_1\mathfrak{I}_3$ has to be taken into account for stabilizing "asymmetric" phases with $\rho_1\neq\rho_2$. Note that the fourth-degree invariants $\rho_1^2\rho_2^2$ and $\rho_1^2\rho_2^2\cos 2\theta$ express at a phenomenological level the exchange striction interactions and anisotropic exchange forces, respectively. Minimizing Φ_1 with respect to θ yields the following equation of state:

$$\rho_1^2\rho_2^2 \sin 2\theta[c_1 + d(\rho_1^2+\rho_2^2) + 2c_2\rho_1^2\rho_2^2\cos 2\theta] = 0. \quad (2)$$

Equation (2) and the equations minimizing Φ_1 with respect to ρ_1 and ρ_2 show that *seven* phases, labeled 1–7, can be stabilized below the P phase for different equilibrium values of ρ_1, ρ_2, and θ. Figure 1 summarizes the equilibrium properties of each phase and their magnetic point-group symmetries, which have been determined following the procedure described by Dvoràk *et al.*[38] One can verify that the phases denoted 2, 4, 6, and 7 display a ferroelectric polarization along y and that all phases correspond to an antiferromagnetic ordering except phase 7 which has a nonzero magnetization along y. The respective location of the phases is indicated in the theoretical phase diagrams shown in Fig. 2, in the space (a_1,b_1,c_1) [Fig. 2(a)] and plane (b_1,c_1) [Fig. 2(b)] of the phenomenological coefficients, and in the orbit space $(\mathfrak{I}_1,\mathfrak{I}_2,\mathfrak{I}_3)$ [Fig. 2(c)]. It allows one to determine the possible sequences of phases separated by second-order transitions as $P\rightarrow1\rightarrow6\rightarrow7$ or $P\rightarrow3\rightarrow4\rightarrow7$. Dielectric and magnetic properties of the phases are deduced from the coupling of the order parameter with the polarization $(\vec{P})$ and magnetization $(\vec{M})$ components, which are $\mathfrak{I}_4=\rho_1\rho_2P_y\sin\theta$, $\mathfrak{I}_5=(\rho_1^2-\rho_2^2)M_xM_y$, and $\mathfrak{I}_6=\rho_1\rho_2M_xM_z\cos\theta$.

The preceding results allow a consistent interpretation of the $P\rightarrow I\rightarrow II$ sequence of phases reported in $TbMn_2O_5$. Phase I observed between T_1 and T_2 corresponds to phase 1

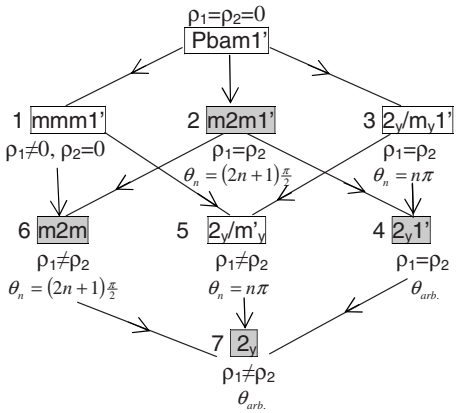

FIG. 1. Connections between the magnetic point groups of phases 1–7 induced by the IC G_1 of Pbam1′, and equilibrium conditions fulfilled by the order parameter in each phase. Gray rectangles indicate ferroelectric phases. $\theta_{arb.}$ stands for arbitrary.

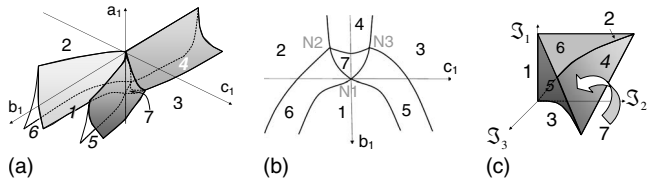

FIG. 2. Phase diagrams deduced from the minimization of the free-energy Φ_1 given by Eq. (1) in (a) the (a_1,b_1,c_1) space, (b) the (b_1,c_1) plane for $a_1<0$, and (c) the orbit space $(\mathfrak{I}_1,\mathfrak{I}_2,\mathfrak{I}_3)$. In (a) the phases are separated by second-order transition surfaces, which become curves in (b). Phases 1, 2, and 3 can be reached directly from the P phase across the second-order plane $a_1=0$. In (b) N1, N2, and N3 are four-phase points, which become curves in (a). In (c) phases (1, 2, 3) and (4, 5, 6) correspond, respectively, to curves and surfaces. Phase 7 coincides with the volume limited by the surfaces (4, 5, 6).

$(\rho_1\neq 0,\ \rho_2=0)$ in Fig. 1. It displays the $mmm1'$ symmetry with antiferromagnetic order in the (x,y) plane $(\mathfrak{I}_5=\rho_1^2M_xM_y)$, a doubling of the lattice parameter a and an incommensurate modulation along c, expressed by the Lifshitz invariant $\rho_1^2\frac{\partial\theta_1}{\partial z}$. Figures 1 and 2 show that a continuous transition can occur from phase 1 to the ferroelectric phase 6 $[\rho_1\neq\rho_2,\ \theta=(2n+1)\frac{\pi}{2}]$, which exhibits a spontaneous polarization along y, and a magnetic symmetry $m2m$ preserving an antiferromagnetic order in the (x,y) plane $(\mathfrak{I}_5\neq 0)$. Identifying phase 6 with phase II of $TbMn_2O_5$ allows a straightforward interpretation of the dielectric behavior observed at the I→II transition. From the dielectric free-energy density $\Phi_1^D=\delta_1\rho_1\rho_2P_y\sin\theta+\frac{P_y^2}{2\epsilon_{yy}^0}$, one gets the equilibrium value of P_y in phase 6

$$P_y^e=\pm\,\delta_1\epsilon_{yy}^0\rho_1\rho_2. \tag{3}$$

The (S_1,S_1^*) components related to ρ_1 have been already activated in phase 1, and *are frozen in phase 6*, which is induced by the sole symmetry-breaking mechanism related to ρ_2. Therefore, Eq. (3) reflects an *effective bilinear coupling* of P_y with ρ_2, giving rise to a *proper ferroelectric* critical behavior at the transition between phases 1 and 6. This situation is reminiscent of *pseudoproper ferroelectric transitions*[23] where the spontaneous polarization has the same symmetry as the transition order parameter, to which it couples bilinearly, but results from an induced mechanism. In phase II of $TbMn_2O_5$, P_y and ρ_2 are related by a *pseudoproperlike* coupling since they display different symmetries. Therefore, at the I→II transition, P_y varies critically as ρ_2, i.e., $P_y\propto(T_2-T)^{1/2}$, whereas the dielectric permittivity ϵ_{yy} exhibits a Curie-Weiss-type divergence $\epsilon_{yy}\propto|T-T_2|^{-1}$. Figures 3(a) and 3(b) show the excellent fit of the experimental curves reported by Hur *et al.*[8] with the preceding power laws. The *induced* character of P_y appears only from its magnitude (40 nC cm^{-2}),[8,9] which is 2 orders smaller than in proper ferroelectrics. Note that a conventional trilinear (improper) coupling between P_y and the magnetic order parameters ρ_1 and ρ_2 would lead to an *upward step* of ϵ_{yy} and to a *linear* dependence of $P_y\propto(T_2-T)$.

At $T_3=33$ K the wave vector locks into the commensurate value $\vec{k}=(\frac{1}{2},0,\frac{1}{4})$. Table I shows that the symmetry of the (S_1,S_1^*,S_2,S_2^*) order parameter is modified at the lock-in transition, the fractional value $k_z=1/4$ changing the translation matrix $(E|00c)$ and giving rise to new (umklapp) invariants $\rho_1^4\cos 4\theta_1+\rho_2^4\cos 4\theta_2$ and $\rho_1^2\rho_2^2\cos 2(\theta_1+\theta_2)$. Taking into account these additional invariants, minimization of Φ_1 yields the equilibrium values $\theta_1=\pm\theta_2=n\frac{\pi}{4}$ for the commensurate phase III, which has the magnetic point-group m2m, and a lattice parameter 4c. The II→III transition coincides with a slight change in the slope of the polarization and no noticeable anomaly of the dielectric permittivity, suggesting a continuous decrease of the k_z component to the commensurate value $\frac{1}{4}$.

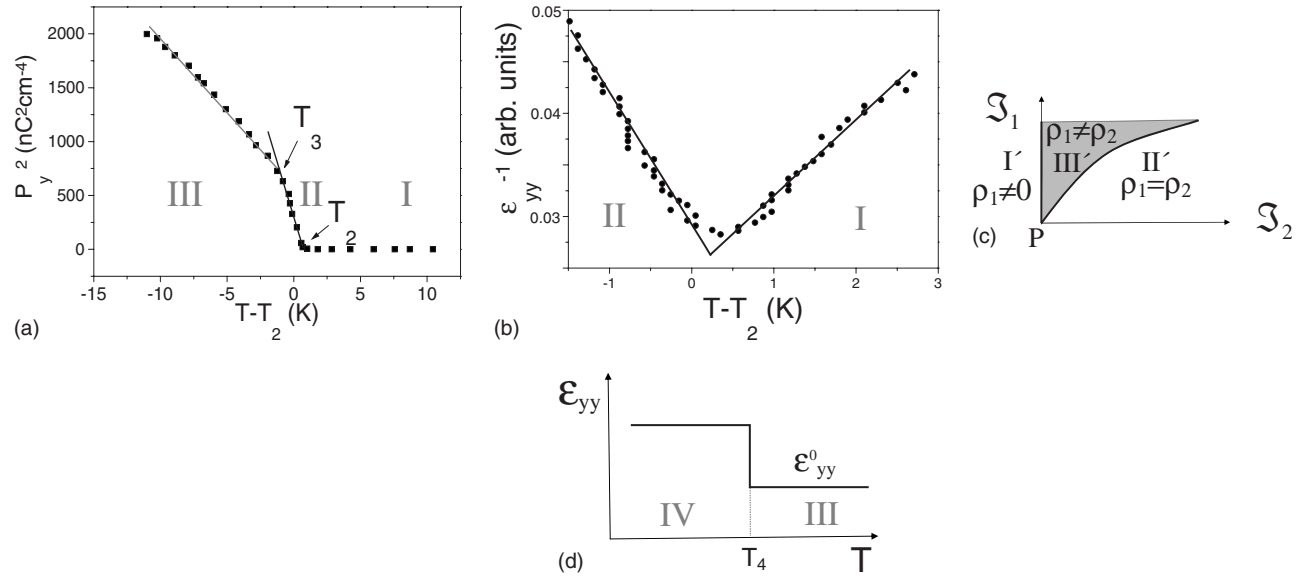

FIG. 3. (a) Least-squares fits for the squared polarization $P_y^2\propto(T_2-T)$ and (b) the inverse dielectric permittivity $\epsilon_{yy}^{-1}\propto|(T_2-T)|$ reported by Hur *et al.* (Ref. 8). (c) Phase diagram associated with Ξ_1 in the orbit space $(\mathfrak{I}_1,\mathfrak{I}_2)$. The magnetic point groups are $2_y/m_y1'$ (phase I′), $mmm1'$ (phase II′), and $2_y'/m_y$ (phase III′). (d) Dielectric permittivity $\epsilon_{yy}(T)$ at the III→IV transition.

Due to the complexity of the magnetic structure of $TbMn_2O_5$ there is no simple connection between the complex amplitudes (S_i, S_i^*) $(i=1,2)$, which span the four-dimensional IC G_1 inducing the $P \rightarrow I \rightarrow II \rightarrow III$ sequence of transitions, and the spin densities associated with the magnetic ions involved in the structure. One can show,[39] for example, that in phase II the spin-density waves corresponding to the magnetic sublattices of Mn^{3+} and Mn^{4+} ions can be expressed as

$$\vec{M}(x_i,z_i) = \cos(kz_i + \tilde{\theta}) \times \left[M_x \cos\left(2x_i - \frac{\pi}{4}\right)\vec{i} + M_y \sin\left(2x_i - \frac{\pi}{4}\right)\vec{j} \right] + M_z \sin(kz_i + \tilde{\theta}) \sin\left(2x_i - \frac{\pi}{4}\right)\vec{k}, \quad (4)$$

with different amplitudes M_x, M_y, and M_z for the two sublattices. $\vec{i}$, $\vec{j}$, and $\vec{k}$ are unit vectors, $\tilde{\theta}=\frac{\theta_1+\theta_2}{2}$, and (x_i,z_i) are coordinates of the Mn^{3+} and Mn^{4+} ions. *Each component of* $\vec{M}$ *transforms as a linear combination of the four-component order parameter* (S_i, S_i^*) used in our phenomenological approach, and the M_x, M_y, and M_z amplitudes are *proportional* to the $\rho_1=\rho_2$ modulus of S_1 and S_2 in phase II.

III. III→IV→V TRANSITIONS

The wave vector $\vec{k}=(k_x,0,k_z)\approx(0.48,0,0.32)$ associated with the III→IV commensurate-incommensurate transition occurring at T_4, corresponds to two four-dimensional IC's of Pbam1′, denoted Ξ_1 and Ξ_2, whose generators are given in Table I. The four-component order parameters spanning the two IC's can be written $(\eta_1=\rho_1 e^{i\phi_1}$, $\eta_1^*=\rho_1 e^{-i\phi_1}$, $\eta_2=\rho_2 e^{i\phi_2}$, $\eta_2^*=\rho_2 e^{-i\phi_2})$ for Ξ_1 and $(\zeta_1=\rho_3 e^{i\phi_3}$, $\zeta_1^*=\rho_3 e^{-i\phi_3}$, $\zeta_2=\rho_4 e^{i\phi_4}$, $\zeta_2^*=\rho_4 e^{-i\phi_4})$ for Ξ_2. It yields the following independent order-parameter invariants: $(\Im_1=\rho_1^2+\rho_2^2$, $\Im_2=\rho_1^2\rho_2^2)$ for Ξ_1, and $(\Im_3=\rho_3^2+\rho_4^2$, $\Im_4=\rho_3^2\rho_4^2)$ for Ξ_2.

Minimization of the free energy associated with Ξ_1 yields three possible stable states, denoted I′, II′, and III′ shown in the $(\Im_1,\Im_2)$ phase diagram of Fig. 3(c), which display the *nonpolar* magnetic symmetries $2_y/m_y1'(\rho_1\neq 0,\rho_2=0)$, $mmm1'(\rho_1=\rho_2)$ and $2_y'/m_y(\rho_1\neq\rho_2\neq 0)$. The same nonpolar symmetries are induced by Ξ_2. Therefore, ferroelectric phases IV and V may only result from a *coupling* of the (η_i) and (ζ_i) order parameters associated with $\Xi_1+\Xi_2$, consistent with the observation by Koo *et al.*[20] of a multiple magnetic ordering in phase IV. Taking into account the coupling invariant $\Im_5=\rho_1^2\rho_3^2\cos 2\Psi_1+\rho_2^2\rho_4^2\cos 2\Psi_2$, with $\Psi_1=\phi_1-\phi_3$ and $\Psi_2=\phi_2-\phi_4$, the free energy associated with $\Xi_1+\Xi_2$ reads

$$\Phi_2(\rho_i,\Psi_i) = \sum_{i=1}^{5} (\alpha_i \Im_i + \beta_i \Im_i^2). \quad (5)$$

Minimization of Φ_2 shows that not less than 15 distinct phases can be stabilized for different equilibrium values of ρ_i and Ψ_i. Six of these phases display a ferroelectric polarization component P_y, resulting from the mixed coupling invariant $\Im_6=P_y(\rho_1\rho_3\sin\Psi_1+\rho_2\rho_4\sin\Psi_2)$. For $\rho_1=\rho_2$, $\rho_3=\rho_4$, $\Psi_1=(2n+1)\frac{\pi}{2}$, or (and) $\Psi_2=(2n+1)\frac{\pi}{2}$ the phases have the magnetic symmetry $m2m$. For $\rho_1\neq 0,\rho_3\neq 0,\rho_2=\rho_4=0$ or $\rho_1=\rho_3=0,\rho_2\neq 0,\rho_4\neq 0$ or $\rho_1\neq\rho_2$, $\rho_3\neq\rho_4$ with Ψ_1 or $\Psi_2=(2n+1)\frac{\pi}{2}$ and Ψ_1 or Ψ_2 arbitrary, or Ψ_1 and Ψ_2 arbitrary, the magnetic symmetry is lowered to 2_y. The magnetic order in the different phases is expressed by the coupling invariants $\Im_7=M_xM_y(\rho_1\rho_3\cos\Psi_1+\rho_2\rho_4\cos\Psi_2)$ and $\Im_8=M_yM_z(\rho_1\rho_3\cos\Psi_1-\rho_2\rho_4\cos\Psi_2)$.

The experimental results reported for the magnetic structure of phase IV of $TbMn_2O_5$ (Ref. 20) are consistent with a magnetic symmetry $m2m$. One can assume, without loss of generality, that the corresponding equilibrium values of the order parameters in phase IV are $\rho_1=\rho_2$, $\rho_3=\rho_4$, $\Psi_1=(2n+1)\frac{\pi}{2}$, and $\Psi_2=n\pi$. Therefore the dielectric contribution to the free energy at the III→IV transition is $\Phi_2^D=\pm\delta_2\rho_1\rho_3P_y+\frac{P_y^2}{2\epsilon_{yy}^0}$. It yields

$$P_y^e = \pm\delta_2\epsilon_{yy}^0\rho_1\rho_3. \quad (6)$$

Since both order parameters ρ_1 *and* ρ_3 contribute to the symmetry-breaking mechanism at T_4, they both vary as $\propto(T_4-T)^{1/2}$ for $T\leq T_4$. Therefore P_y varies linearly as (T_4-T), which expresses a typical improper ferroelectric behavior for the III→IV transition. The dielectric permittivity is given by $\epsilon_{yy}=\epsilon_{yy}^0(1-\delta_2\frac{\partial\rho_1\rho_3}{\partial E_y})$, where E_y is the applied electric field. It yields $\epsilon_{yy}=\epsilon_{yy}^0$ for $T>T_4$, and $\epsilon_{yy}\approx\frac{\epsilon_{yy}^0}{1-\delta_2^2\epsilon_{yy}^0 f(\beta_i,\alpha_5)}$ for $T<T_4$, where $f(\beta_i,\alpha_5)$ represents a combination of phenomenological coefficients of Φ_2 with $0<f(\beta_i,\alpha_5)<1$. Accordingly, $\epsilon_{yy}(T)$ undergoes an upward step at T_4 [Fig. 3(d)], as observed experimentally.[8,9] Note that the change in the order-parameter symmetry imposes a first-order character to the III→IV transition, consistent with the lattice anomalies observed at 24 K.[9].

The preceding description allows a straightforward explanation of the observed decrease[8] in the equilibrium polarization P_y^e at zero magnetic field which is starting at about 26 K. Below T_4, P_y^e is the sum of two distinct contributions given by Eqs. (3) and (6).

$$P_y^e = \pm\epsilon_{yy}^0[\delta_1\rho_1(T_2-T)^{1/2}+\delta_2(T_4-T)], \quad (7)$$

where $\rho_1\propto(T_1-T_2)^{1/2}$. Assuming $\delta_1>0$ and $\delta_2<0$, one can verify that P_y^e decreases for $T\leq T_{\max}=T_2-\frac{\delta_1^2(T_1-T_2)}{4\delta_2^2}$. This explanation confirms the conjecture by Hur *et al.*[8] that the total polarization is composed of positive and negative components, which appear at T_2 and T_4, respectively. The opposite signs of P_y^e in Eq. (7) correspond to the opposite ferroelectric domains disclosed by the preceding authors under opposite electric fields. The strong increase in P_y^e observed below T_5 reflects the positive contribution of phase V to the total polarization. The absence of a dielectric anomaly at T_5 suggests that the $m2m$ symmetry of phase IV remains unchanged in phase V with an eventual change in the respective values of Ψ_1 or (and) Ψ_2.

It remains to understand why the decrease in P_y is enhanced by application of a magnetic field H_x, leading to a change in sign of P_y above a threshold field H_x^c.[8,9] This can be explained by considering the magnetic and magnetoelec-

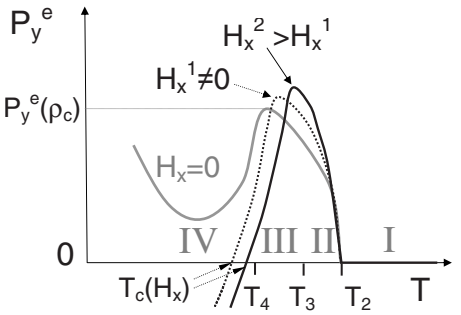

FIG. 4. Temperature dependence of $P_y^e(T,H_x)$ given by Eq. (9), for $\delta_1>0$, $\delta_2<0$, $\nu<0$. With increasing field $P_y^e(T,H_x)$ decreases more sharply and is shifted to higher temperature. The change in sign of $P_y^e(T,H_x)$ occurs at a field-dependent critical temperature $T_c(H_x)$.

tric contributions to the free energy under H_x field in phase IV: $\Phi_2^M=\mu_0\frac{M_x^2}{2}-H_xM_x$ and $\Phi_2^{ME}=\nu\rho_1\rho_3P_yM_x^2$. It yields for the field dependent spontaneous polarization in phase IV

$$P_y^{\mathrm{IV}}(H_x)=\pm\epsilon_{yy}^0\rho_1\rho_3(\delta_2+\nu\mu_0^{-2}H_x^2). \tag{8}$$

For $\nu<0$ the application of an H_x field enhances the negative contribution P_y^{IV} to the temperature dependence of the total polarization leading to

$$P_y^e(T,H_x)=\pm\epsilon_{yy}^0[\delta_1(T_1-T_2)^{1/2}(T_2-T)^{1/2}+(\delta_2+\nu\mu_0^{-2}H_x^2)(T_4-T)]. \tag{9}$$

Accordingly $P_y^e(T,H_x)$ changes sign for the temperature dependent threshold field,

$$H_x^c(T)^2=-\frac{\mu_0^2}{\nu}\left[\delta_2+\frac{\delta_1(T_1-T_2)^{1/2}(T_2-T)^{1/2}}{(T_4-T)}\right]. \tag{10}$$

From Eqs. (9) and (10) one can verify that with increasing applied field, $P_y^e(T,H_x)$ decreases more sharply and changes sign at higher temperature (Fig. 4), as was actually observed by Hur *et al.*[8]

IV. SUMMARY AND DISCUSSION

In summary, it has been shown that two distinct symmetry-breaking ordering parameters are involved in the sequence of five magnetic phases found in $TbMn_2O_5$ below $T_1=43$ K: (1) A single four-component order parameter is associated with the $P\rightarrow I\rightarrow II\rightarrow III$ transitions. Two among the components (S_1,S_1^*) give rise at T_1 to the antiferromagnetic phase I, whereas the two others (S_2,S_2^*) are activated at T_2, at the onset of the ferroelectric phase II, (S_1,S_1^*) being frozen at the $I\rightarrow II$ transition. It results in a hybrid pseudoproper ferroelectric behavior for this transition, which displays critical dielectric anomalies typical of proper ferroelectric transitions, although the magnitude of the induced polarization in phase II is of the order found in improper ferroelectrics. At the $II\rightarrow III$ transition the translational symmetry along z becomes commensurate, modifying in a minor way the ferroelectric properties of the material. The theoretical phase diagram showing the location of the phases stabilized in $TbMn_2O_5$, as well as the other five phases induced by the (S_i,S_i^*) order parameter, has been worked out, and the magnetic point groups of the different phases have been given.

(2) At the commensurate-incommensurate $III\rightarrow IV$ transition the (S_i,S_i^*) order parameter splits into two distinct four-component order parameters (η_i) and (ζ_i), which couple for inducing the ferroelectric phases IV and V. The $III\rightarrow IV$ transition shows a standard improper ferroelectric behavior. The absence of a noticeable anomaly for the dielectric permittivity at the $IV\rightarrow V$ transition suggests that the structural symmetry of phase IV remains unchanged in phase V. However, the spontaneous polarization in phase V contributes positively to the observed total polarization P_y^e, whereas phase IV exhibits a negative contribution to P_y^e. Opposite signs of the spontaneous electric polarizations in phases IV and V provide a consistent interpretation of the nonmonotonous temperature dependence of $P_y^e(T)$ across the $II\rightarrow III\rightarrow IV\rightarrow V$ sequence of induced ferroelectric transitions. Application of an H_x magnetic field modifies the preceding behavior, via the magnetoelectric coupling between P_y and the induced magnetization M_x, which contributes negatively to the total polarization, explaining the observed change in sign of $P_y^e(T,H_x)$.

A number of previous studies[24–30] proposed a theoretical description of the dielectric and magnetoelectric properties of $TbMn_2O_5$. However, these studies did not take fully into account the order-parameter symmetries associated with the different phases. Therefore, the relevant free energies, expanded to the necessary degrees, and the related coupling terms could not be disclosed, and the proper phase diagrams could not be derived. As a consequence, a consistent interpretation of the dielectric behavior at zero magnetic field, or under applied H_x field, could not be given explicitly. In contrast to our phenomenological description, based on the symmetry and thermodynamic considerations underlying the Landau theory of magnetic phase transitions,[21–23] which is free from any microscopic model, the previous works, using different group-theoretical procedures, attempted to deduce the magnetoelectric properties of the material from its complex magnetic structures and related magnetic interactions. For example, Radaelli and Chapon limit their group-theoretical analysis to the irreducible corepresentations of the little group.[24] It does not allow determination of the transition free energy and of the coupling relating the polarization to the magnetic order parameter, which they deduce from microscopic coupling mechanisms.[25] The group-theoretical procedure proposed by Harris[26] for determining the transition order parameter from the spin configuration of $TbMn_2O_5$ does not provide the relevant order-parameter symmetry, and is not related organically with the different effective free energies used by Harris *et al.*[27,28] for describing the ferroelectric transitions in this material. It leads to oversimplified phase diagrams and to a speculative interpretation of the observed dielectric and magnetoelectric properties. Besides, the critical wave vector assumed by Harris *et al.*[27] for phases I and II of $TbMn_2O_5$ corresponds actually to phases IV and V. The Landau model used by Kadomtseva *et al.*[29] provides an insight into the exchange and relativistic magnetic contributions to the free energy and induced polar-

ization involved in $R\mathrm{Mn_2O_5}$ compounds. However, the dimensionality of the irreducible representation and order parameter assumed in their model (two dimensional instead of two coupled four-dimensional order parameters required for $\mathrm{ErMn_2O_5}$ and $\mathrm{YMn_2O_5}$), and the fact that two successive and distinct order parameters are needed for describing the full sequence of observed phases, do not allow these authors to describe the observed dielectric properties and magnetoelectric effects. Along another line, the model proposed by Sushkov *et al.*[30] provides an interesting analysis of the underlying magnetic forces explaining the induced dielectric properties in the $R\mathrm{Mn_2O_5}$ family, but a detailed description of the observed phase sequences and magnetoelectric effects, which would require considering the actual order-parameter symmetries, is missing.

Similar sequences of ferroelectric phases are found in other $R\mathrm{Mn_2O_5}$ compounds[31–36] where $R=\mathrm{Bi,Y}$ or a rare-earth heavier than Nd. In these compounds, with the exception of $\mathrm{BiMn_2O_5}$, the first ferroelectric phase does not appear directly below the paramagnetic phase, but below an intermediate nonpolar antiferromagnetic phase. Therefore the induced electric polarization results from the coupling of two distinct magnetic order parameters, one of which having been already activated in the intermediate phase. As a consequence a pseudoproper coupling is created, which gives rise to the typical critical behavior of a proper ferroelectric transition. In $\mathrm{TbMn_2O_5}$ the first ferroelectric transition corresponds to $\vec{k}=(\frac{1}{2},0,k_z)$ and to a *single* four-component order parameter, the pseudoproper coupling occurring between *distinct components* of the same order parameter. A different situation is found in the other $R\mathrm{Mn_2O_5}$ compounds, in which the first transitions correspond to $\vec{k}=(k_x,0,k_z)$,[31–36] i.e., the pseudoproper coupling occurs between *two distinct four-component order parameters* having the symmetries of the (η_i) and (ζ_i) order parameters, which are associated in the present work to the lower temperature transition sequence of $\mathrm{TbMn_2O_5}$. The order parameters involved in the $R\mathrm{Mn_2O_5}$ family correspond in most cases to the symmetries disclosed in the present work for $R=\mathrm{Tb}$, i.e., to $\vec{k}=(\frac{1}{2},0,k_z)$, $(k_x,0,k_z)$, and $(\frac{1}{2},0,\frac{1}{4})$. Two exceptions are presently known, which are:

(1) The lower temperature phase of $\mathrm{DyMn_2O_5}$ (Ref. 35) induced by bidimensional order parameters corresponding to the wave vector $(\frac{1}{2},0,0)$, and

(2) The single ferroelectric phase of $\mathrm{BiMn_2O_5}$ (Ref. 36) induced by bidimensional IC's at $\vec{k}=(\frac{1}{2},0,\frac{1}{2})$.

Accordingly, despite the apparent variety of behaviors found for the dielectric properties and field effects a unifying theoretical framework can be proposed for the $R\mathrm{Mn_2O_5}$ manganites,[39] which can be deduced from the description given in the present work, by interchanging the order parameters in the observed transition sequences.

V. CONCLUSION

In conclusion, the order-parameter symmetries associated with the magnetostructural transitions observed in $\mathrm{TbMn_2O_5}$ clarify the nature of the ferroelectric phases and permit a consistent description of the magnetoelectric effects observed in this material. In a more general way, our phenomenological approach illustrates the necessity of taking into account the actual order-parameter symmetries and phase diagrams associated with the phase sequences reported in multiferroic compounds. This approach can be used for analyzing the microscopic mechanisms and interactions in $R\mathrm{Mn_2O_5}$ manganites,[39] which have not been discussed in the present work.

ACKNOWLEDGMENTS

Support by the Austrian FWF (Grant No. P19284-N20) and by the University of Vienna within the IC Experimental Materials Science ("Bulk Nanostructured Materials") is gratefully acknowledged.

[1] T. Kimura, T. Goto, H. Shintani, K. Ishizaka, T. Arima, and Y. Tokura, Nature (London) **426**, 55 (2003).
[2] T. Kimura, Annu. Rev. Mater. Res. **37**, 387 (2007).
[3] M. Fiebig, J. Phys. D **38**, R123 (2005).
[4] W. Eerenstein, N. D. Mathur, and J. F. Scott, Nature (London) **442**, 759 (2006).
[5] R. Ramesh and N. A. Spaldin, Nature Mater. **6**, 21 (2007).
[6] S.-W. Cheong and M. Mostovoy, Nature Mater. **6**, 13 (2007).
[7] T. Goto, T. Kimura, G. Lawes, A. P. Ramirez, and Y. Tokura, Phys. Rev. Lett. **92**, 257201 (2004).
[8] N. Hur, S. Park, P. A. Sharma, J. S. Ahn, S. Guha, and S.-W. Cheong, Nature (London) **429**, 392 (2004).
[9] L. C. Chapon, G. R. Blake, M. J. Gutmann, S. Park, N. Hur, P. G. Radaelli, and S.-W. Cheong, Phys. Rev. Lett. **93**, 177402 (2004).
[10] G. Lawes, A. B. Harris, T. Kimura, N. Rogado, R. J. Cava, A. Aharony, O. Entin-Wohlman, T. Yildrim, M. Kenzelmann, C. Broholm, and A. P. Ramirez, Phys. Rev. Lett. **95**, 087205 (2005).
[11] K. Taniguchi, N. Abe, T. Takenobu, Y. Iwasa, and T. Arima, Phys. Rev. Lett. **97**, 097203 (2006).
[12] K. Tomiyasu, J. Fukunaga, and H. Suzuki, Phys. Rev. B **70**, 214434 (2004).
[13] R. E. Newnham, J. J. Kramer, W. A. Schulze, and L. E. Cross, J. Appl. Phys. **49**, 6088 (1978).
[14] H. Katsura, N. Nagaosa, and A. V. Balatsky, Phys. Rev. Lett. **95**, 057205 (2005).
[15] M. Mostovoy, Phys. Rev. Lett. **96**, 067601 (2006).
[16] I. A. Sergienko and E. Dagotto, Phys. Rev. B **73**, 094434 (2006).
[17] M. Kenzelmann, A. B. Harris, S. Jonas, C. Broholm, J. Schefer, S. B. Kim, C. L. Zhang, S.-W. Cheong, O. P. Vajk, and J. W. Lynn, Phys. Rev. Lett. **95**, 087206 (2005).
[18] J. Hu, Phys. Rev. Lett. **100**, 077202 (2008).
[19] G. R. Blake, L. C. Chapon, P. G. Radaelli, S. Park, N. Hur, S.-W. Cheong, and J. Rodriguez-Carvajal, Phys. Rev. B **71**, 214402 (2005).

[20] J. Koo, C. Song, S. Ji, J.-S. Lee, J. Park, T.-H. Jang, C.-H. Yang, J.-H. Park, Y. H. Jeong, K.-B. Lee, T. Y. Koo, Y. J. Park, J.-Y. Kim, D. Wermeille, A. I. Goldman, G. Srajer, S. Park, and S.-W. Cheong, Phys. Rev. Lett. **99**, 197601 (2007).
[21] L. D. Landau, Zh. Eksp. Teor. Fiz. **7**, 627 (1937).
[22] I. E. Dzialoshinskii, Sov. Phys. JETP **19**, 960 (1964).
[23] J. C. Tolédano and P. Tolédano, *The Landau Theory of Phase Transitions* (World Scientific, Singapore, 1987).
[24] P. G. Radaelli and L. C. Chapon, Phys. Rev. B **76**, 054428 (2007).
[25] P. G. Radaelli and L. C. Chapon, J. Phys.: Condens. Matter **20**, 434213 (2008).
[26] A. B. Harris, Phys. Rev. B **76**, 054447 (2007).
[27] A. B. Harris, A. Aharony, and O. Entin-Wohlman, J. Phys.: Condens. Matter **20**, 434202 (2008).
[28] A. B. Harris, M. Kenzelmann, A. Aharony, and O. Entin-Wohlman, Phys. Rev. B **78**, 014407 (2008).
[29] A. M. Kadomtseva, S. S. Krotov, Yu. F. Popov, G. P. Vorob'ev, and M. M. Lukina, J. Exp. Theor. Phys. **100**, 305 (2005).
[30] A. B. Sushkov, M. Mostovoy, R. Valdés Aguilar, S.-W. Cheong, and H. D. Drew, J. Phys.: Condens. Matter **20**, 434210 (2008).
[31] Y. Noda, H. Kimura, M. Fukunaga, S. Kobayashi, I. Kagomiya, and K. Kohn, J. Phys.: Condens. Matter **20**, 434206 (2008).
[32] L. C. Chapon, P. G. Radaelli, G. R. Blake, S. Park, and S.-W. Cheong, Phys. Rev. Lett. **96**, 097601 (2006).
[33] Y. Bodenthin, U. Staub, M. Garcia-Fernandez, M. Janoschek, J. Schlappa, E. I. Golovenchits, V. A. Sanina, and S. G. Lushnikov, Phys. Rev. Lett. **100**, 027201 (2008).
[34] D. Higashiyama, S. Miyasaka, and Y. Tokura, Phys. Rev. B **72**, 064421 (2005).
[35] N. Hur, S. Park, P. A. Sharma, S. Guha, and S.-W. Cheong, Phys. Rev. Lett. **93**, 107207 (2004).
[36] A. Munoz, J. A. Alonso, M. T. Casais, M. J. Martinez-Lope, J. L. Martinez, and M. T. Fernandez-Diaz, Phys. Rev. B **65**, 144423 (2002).
[37] P. Tolédano and V. Dmitriev, *Reconstructive Phase Transitions* (World Scientific, Singapore, 1996).
[38] V. Dvorák, V. Janovec, and Y. Ishibashi, J. Phys. Soc. Jpn. **52**, 2053 (1983).
[39] B. Mettout and P. Tolédano (unpublished).
[40] O. V. Kovalev, *The Irreducible Representation of Space Groups* (Gordon and Breach, New York, 1965).